Density Functional Investigation of the Difference in the Magnetic Structures of the Layered Triangular Antiferromagnets CuFeO 2 and AgCrO 2

ARTICLE *in* CHEMISTRY OF MATERIALS · AUGUST 2011

Impact Factor: 8.35

3 AUTHORS:

Yuemei Zhang

University of California, Riverside

22 PUBLICATIONS **278** CITATIONS

SEE PROFILE

Erjun Kan

Nanjing University of Science and Technology

102 PUBLICATIONS **1,612** CITATIONS

SEE PROFILE

Myung-Hwan Whangbo

North Carolina State University

704 PUBLICATIONS **14,990** CITATIONS

SEE PROFILE

CHEMISTRY OF MATERIALS

ARTICLE

pubs.acs.org/cm

Density Functional Investigation of the Difference in the Magnetic Structures of the Layered Triangular Antiferromagnets $CuFeO_2$ and $AgCrO_2$

Yuemei Zhang,[†] Erjun Kan,[‡] and Myung-Hwan Whangbo*[,†]

[†]Department of Chemistry, North Carolina State University, Raleigh, North Carolina 27695-8204, United States

[‡]Department of Applied Physics, Nanjing University of Science and Technology, Nanjing, Jiangsu 210094, P. R. China

ABSTRACT: The layered triangular antiferromagnets $CuFeO_2$ and $AgCrO_2$ exhibit ferroelectric polarization when they adopt a helical spiral-spin magnetic structure. Application of magnetic field parallel to the *c*-axis or doping Fe sites with Al or Ga is necessary for $CuFeO_2$ to have a helical spiral spin order. However, $AgCrO_2$ adopts a helical spiral spin order in the absence of such extrinsic factors. A probable cause for this difference between the two systems was examined by evaluating the relative stabilities of their helical spiral and collinear spin structures on the basis of density functional calculations. In contrast to the case of $AgCrO_2$, the collinear ↑↑↓↓ state is only slightly higher in energy than the helical spiral-spin state Q_{a+b} in $CuFeO_2$ so that extrinsic factors such as oxygen vacancy and applied magnetic field can influence whether $CuFeO_2$ adopts the ↑↑↓↓ or Q_{a+b} structure.

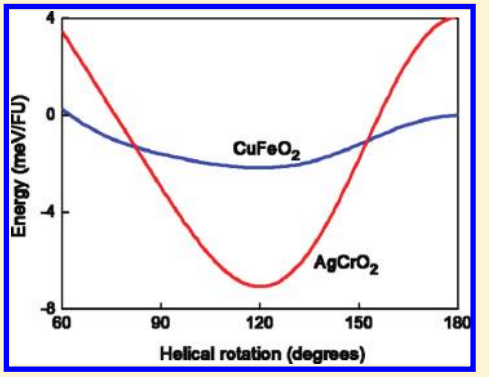

KEYWORDS: layered triangular antiferromagnet, $CuFeO_2$, ferroelectricity, spiral spin, spin exchange, density functional analysis

1. INTRODUCTION

Multiferroic (i.e., magnetic ferroelectric) materials have received much attention due to the potential of controlling their physical properties by either magnetic or electric field.[1] A centrosymmetric crystalline solid can become ferroelectric (FE) when it loses inversion symmetry, which is often induced either by cooperative Jahn−Teller distortion[1b,2] or by chiral magnetic order.[1f,3] The FE polarization driven by magnetic order has been discussed in terms of exchange striction[4] or spin−orbit coupling (SOC).[5] The layered triangular antiferromagnets such as $CuFeO_2$[6] and $AgCrO_2$[7] exhibit FE polarization when their magnetic structure acquires a helical spiral-spin order in the chains of M^{3+} (M = Fe, Cr) ions of their MO_2 layers. The MO_2 layers of AMO_2 (A = Cu, M = Fe; A = Ag, M = Cr) are made up of edge-sharing MO_6 octahedra[8,9] containing high-spin M^{3+} (d^5, S = 5/2 for M = Fe; d^3, S = 3/2 for M = Cr) ions (Figure 1a).[10] Each MO_2 layer can be viewed in terms of the MO_4 chains of edge-sharing FeO_6 octahedra running along the a-, b-, or (a+b)-direction. Adjacent MO_2 layers of AMO_2 are stacked along the c-direction with A^+ (d^{10}) ions intercalated between the MO_2 layers to form linear O−A−O bridges (Figure 1b) such that there are three MO_2 layers per unit cell. Although $CuFeO_2$ and $AgCrO_2$ are similar in crystal structure, they show an interesting difference in magnetic structure. The magnetic ground state of $CuFeO_2$ has the ↑↑↓↓ spin arrangement in each FeO_2 layer (Figure 2a) with their spins parallel to the *c*-axis.[11] This magnetic structure is modified by magnetic field **H** applied along the c-direction; the magnetic structure changes from the ↑↑↓↓ arrangement under **H** < ~7 T to the helical spiral-spin structure under **H** ≈ 7−13 T to the ↑↑↑↓ structure (Figure 2b) under **H** > ~13 T.[6a,12] The helical spiral-spin state can also be induced into $CuFeO_2$ without applying magnetic field by doping the Fe

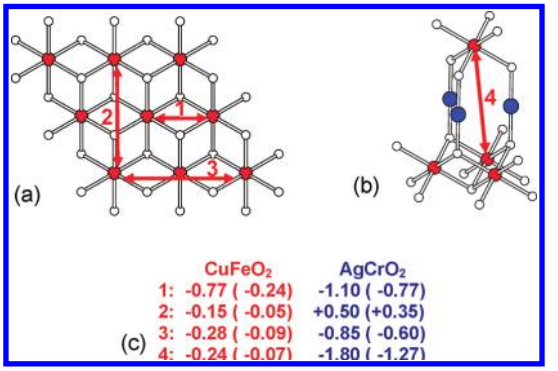

Figure 1. (a) An isolated FeO_2 layer of $CuFeO_2$ made of edge-sharing FeO_6 octahedra showing the intralayer spin exchange paths J_1, J_2, and J_3. (b) A zoomed-in view of how two adjacent FeO_2 layers of $CuFeO_2$ are linked by O−Cu−O bridges showing the interlayer spin exchange J_4. The Fe, Cu, and O atoms are indicated by red, blue, and white circles, respectively. The numbers 1−4 in (a, b) refer to the spin exchange paths J_1−J_4, respectively. (c) The values of J_1−J_4 (in meV) found for $CuFeO_2$ and $AgCrO_2$ obtained from GGA+U calculations. The numbers outside the parentheses are the as-calculated values, and those inside the parentheses are the reduced values using the overestimation factor f = 3.24 for $CuFeO_2$ and f = 1.42 for $AgCrO_2$ (see the text for details).

Received: April 22, 2011
Revised: August 24, 2011

   dx.doi.org/10.1021/cm2011567 | *Chem. Mater.* XXXX, XXX, 000–000

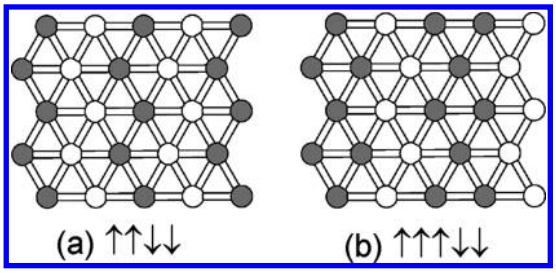

Figure 2. The collinear magnetic structures of $CuFeO_2$ below 10 K under magnetic field: (a) the ↑↑↓↓ structure under magnetic field lower than ~7 T and (b) the ↑↑↑↓↓ structure under magnetic field greater than ~13 T. The filled and empty circles represent the spins of the Fe^{3+} ions that are aligned along the positive and negative *c*-axis directions, respectively.

sites with Al or Ga atoms.[6b,13] In contrast, $AgCrO_2$ adopts a helical spiral-spin state in the absence of applied magnetic field **H**.

The magnetic structure of $CuFeO_2$ at low temperature was examined by inelastic neutron scattering measurements,[14] and the resulting spin wave dispersion relations were theoretically analyzed[15] to find that the three intralayer spin exchanges J_1−J_3 and the interlayer spin exchange J_4 (Figure 1) are all antiferromagnetic. Other magnetic properties of $CuFeO_2$ were also investigated in a number of studies.[16] So far, however, it has not been explained why $CuFeO_2$ requires a magnetic field applied parallel to the *c*-axis to adopt a helical spiral spin order, but $AgCrO_2$ does not. To answer this question, one needs to estimate the relative energies of the collinear and helical spiral spin states of $CuFeO_2$ and $AgCrO_2$, which in turn requires the knowledge of their spin exchange interactions. The spin exchange parameters of $CuFeO_2$ were deduced experimentally,[14,15] but those of $AgCrO_2$ were not. In contrast, the spin exchange parameters of $AgCrO_2$ were evaluated on the basis of density functional theory (DFT) calculations,[7b] but those of $CuFeO_2$ were not.

In the present work, we examine the difference in the magnetic structures of $CuFeO_2$ and $AgCrO_2$ on the basis of DFT calculations. We first evaluate the spin exchange parameters of $CuFeO_2$ by performing DFT calculations and then determine the relative stabilities of the helical spiral and collinear spin structures of $CuFeO_2$ and $AgCrO_2$ in terms of their spin exchange parameters and finally propose a most-likely reason why $CuFeO_2$ and $AgCrO_2$ differ in their magnetic structures under magnetic field.

2. DETAILS OF CALCULATIONS

Our spin-polarized DFT calculations employed the projector augmented wave method[17] coded in the Vienna ab initio simulation package,[18] the generalized gradient approximation (GGA) for the exchange and correlation corrections,[19] and the plane wave cutoff energies of 500 and 400 eV for the calculations without and with including the effect of SOC, respectively. To describe the electron correlation associated with the Fe 3d states, the GGA plus on-site repulsion U (GGA+U) method was applied with an effective U = 4 eV on the Fe atom. As in the case of $AgCrO_2$,[7b] we consider the four spin exchange interactions J_1−J_4 defined in Figure 1 and evaluate their values by performing GGA+U calculations for the five ordered spin states of $CuFeO_2$ defined in Figure 3.

3. SPIN EXCHANGE INTERACTIONS

We determine the four spin exchange parameters J_1−J_4 of $CuFeO_2$ (Figure 1) by performing mapping analysis[20] on the

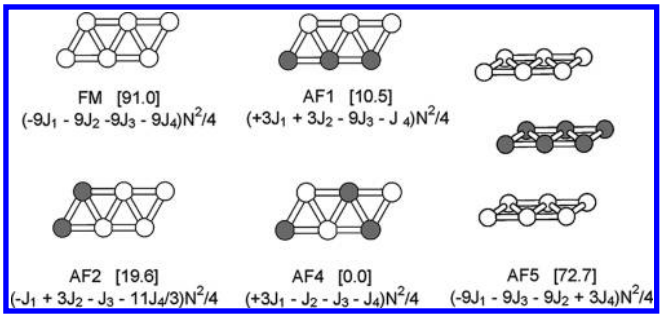

Figure 3. The five ordered spin states of $CuFeO_2$ constructed using a (3a, 2b, c) supercell, where the filled and empty circles represent up-spin and down-spin Fe^{3+} sites, respectively. In (a−d), all three FeO_2 layers of the (3a, 2b, c) supercell have the same spin arrangement, so that the spin arrangement of only one FeO_2 layer is shown. In (e), the spins are ferromagnetic in each FeO_2 layer, but the (3a, 2b, c) supercell consists of one up-spin and two down-spin layers. For each state, the number in each square bracket refers to the relative energy per three FUs determined from GGA+U calculations, and the energy expression to the total spin exchange energy per three FUs with $N = 5$.

basis of the five ordered spin states (FM, AF1, AF2, AF3, AF4) shown in Figure 3. The relative energies, per three formula units (FUs), of these states were determined from our GGA+U calculations as summarized in Figure 3. The energies of these states can also be described in terms of the spin Hamiltonian,

$$\hat{H} = -\sum_{i<j} J_{ij}\hat{S}_i \cdot \hat{S}_j \qquad (1)$$

where J_{ij} (= J_1−J_4) is the spin exchange parameter for the spin exchange interaction between the spin sites i and j. By applying the energy expressions obtained for spin dimers with *N* unpaired spins per spin site ($N = 5$ for $CuFeO_2$),[20] the total spin exchange energies of the five ordered spin states (per three FUs) are written as summarized in Figure 3. Thus, by mapping the relative energies of the five ordered spin states determined by the GGA +U calculations onto the corresponding relative energies determined from the above spin exchange energies, we obtain the values of J_1−J_4 summarized in Figure 1c, where the corresponding values of $AgCrO_2$[7b] are also listed for comparison. (To compare the spin exchange interactions of $CuFeO_2$ with those of $AgCrO_2$, it is necessary to use the effective spin exchanges $J_i^{eff} = S^2 J_i$, where S = 5/2 and 3/2 for $CuFeO_2$ and $AgCrO_2$, respectively.)

Figure 1c shows that the intralayer exchanges J_1 and J_3 as well as the interlayer exchange J_4 of $CuFeO_2$ are substantially antiferromagnetic (AFM), namely, J_1−J_4 = −0.77, − 0.15, −0.28, and −0.24 meV, respectively. These values are the same in sign as, and are comparable in magnitude to, the corresponding spin exchanges deduced from the inelastic neutron scattering measurements (namely, −0.45, −0.20, −0.26, and −0.13 meV, respectively).[14] In each FeO_2 layer, spin frustration[21] occurs in the (J_1, J_1, J_1) and (J_3, J_3, J_3) triangles and in the (J_1, J_1, J_3) line segments. Between adjacent FeO_2 layers, spin frustration occurs in the isosceles (J_1, J_4, J_4) triangles. That is, both the intralayer and the interlayer interactions are spin-frustrated in $CuFeO_2$, as found for $AgCrO_2$.[7b] The spin exchange interactions of $CuFeO_2$ differ from those of $AgCrO_2$ in two aspects: (a) Among J_1−J_4, the AFM interlayer spin exchange J_4 is the strongest interaction in $AgCrO_2$ but is quite weak in $CuFeO_2$, and (b) the intralayer exchange J_2 is ferromagnetic (FM) in $AgCrO_2$ but is AFM in

dx.doi.org/10.1021/cm2011567 |*Chem. Mater.* XXXX, XXX, 000–000

$CuFeO_2$. As discussed in the next section, these two differences are important in explaining why a magnetic field applied parallel to the *c*-axis is necessary for $CuFeO_2$ to adopt the helical spiral-spin structure while this is not the case for $AgCrO_2$.

It is known that GGA+U electronic structure calculations generally overestimate the magnitude of spin exchange interactions.[22] To find the overestimation factors *f* for the calculated spin exchange parameters of $CuFeO_2$ and $AgCrO_2$ (Figure 1c), we calculate their Curie−Weiss temperatures θ using the mean field approximation,[23] namely,

$$\theta = \frac{S(S+1)}{3k_B}\sum_i z_i J_i \qquad (2)$$

where the summation runs over all nearest neighbors of a given spin site, z_i is the number of nearest neighbors connected by the spin exchange parameter J_i, and S is the spin quantum number of each spin site (i.e., S = 5/2 for Fe^{3+} in $CuFeO_2$ and S = 3/2 for Cr^{3+} in $AgCrO_2$). Thus, for $CuFeO_2$ and $AgCrO_2$, θ can be approximated by

$$\theta \approx 2S(S+1)(J_1 + J_2 + J_3 + J_4)/k_B \qquad (3)$$

The as-calculated J_1−J_4 values of Figure 1c lead to θ = −292 and −283 K for $CuFeO_2$ and $AgCrO_2$, respectively, while the corresponding experimental values are −90[24] and −200 K,[25] respectively. Thus, according to the experimental Curie−Weiss temperatures and the mean-field theory, the as-calculated J_1−J_4 values are overestimated by a factor of *f* = 3.24 and 1.42 for $CuFeO_2$ and $AgCrO_2$, respectively. Figure 1c also lists, in parentheses, the values of J_1−J_4 reduced using the overestimation factor *f*. For $CuFeO_2$, the reduced J_1−J_4 values are −0.24, − 0.05, −0.09, and −0.07 meV, respectively, which are smaller in magnitude than the corresponding values deduced from the inelastic neutron scattering measurements[14] (see above) approximately by a factor of 2.

4. RELATIVE STABILITIES OF THE HELICAL SPIRAL AND COLLINEAR SPIN STRUCTURES

To probe why a magnetic field applied parallel to the *c*-axis is needed for $CuFeO_2$ to acquire a helical spiral-spin structure, we first determine the magnetic anisotropy of $CuFeO_2$ by performing GGA+U+SOC calculations for its ↑↑↓↓ state. These calculations reveal that the spin orientation parallel to the *c*-axis (//c) is more stable than that perpendicular to the *c*-axis (⊥c) by 0.12 meV per FU; namely, the magnetic anisotropy of each Fe^{3+} (S = 5/2) ion is very weak. This is not surprising because, to a first approximation, L = 0 for the Fe^{3+} ion in each FeO_6 octahedron so that the effect of SOC should be weak. This suggests that the spin orientation of $CuFeO_2$ might be easily influenced by extrinsic factors such as oxygen vacancy and applied magnetic field.

Since $CuFeO_2$ can switch from the ↑↑↓↓ state to the helical spiral-spin state depending on the strength of applied magnetic field **H** < ∼13 T, the two states should be close in energy. (Note that 1 T is equivalent to 0.67 K.) Such a field-dependence is not known for $AgCrO_2$, which adopts the helical spiral-spin state, thereby implying that the ↑↑↓↓ state is much less stable than the helical spiral-spin state in $AgCrO_2$. To verify these implications, we examine the relative stabilities of several helical spiral and collinear spin states of $CuFeO_2$ and $AgCrO_2$ in terms of their spin exchange parameters J_1−J_4. In estimating the relative stabilities of these states, we employ the reduced J_1−J_4 values obtained from the as-calculated values by the overestimation factor *f*. However, the use of the as-calculated J_1−J_4 values leads essentially to the same conclusion. As a representative example of the helical spiral-spin structure, we consider the helical spiral-spin structure Q_{a+b} = (q, q) as a function of the helical rotation angle θ = q × 360° (q = 1/5, 1/4, 1/3, 1/2). In Q_{a+b} = (1/3, 1/3), for example, the helical spiral-spin chains run along the positive a-direction with clockwise helical-rotation of 120°, and the spiral-spin chains repeat along the positive b-direction while advancing the helical-rotation clockwise by 120°. In terms of J_1−J_4, the energy $E(\theta)$ of the Q_{a+b} structure as a function of θ is written as

$$\begin{aligned} E(\theta) = \{ &-3J_1[2\cos\theta + \cos 2\theta] \\ &-3J_2[1 + 2\cos 3\theta] - 3J_3[2\cos 2\theta + \cos 4\theta] \\ &-J_4[3 + 4\cos\theta + 2\cos 2\theta]\}(N^2/4) \end{aligned} \qquad (4)$$

The $E(\theta)$ vs θ plots calculated for $CuFeO_2$ and $AgCrO_2$ using their spin exchange parameters (reduced by the overestimation factor *f*) are presented in Figure 4 in the region of θ = 60 − 180° (i.e., q = 1/6 − 1/2).

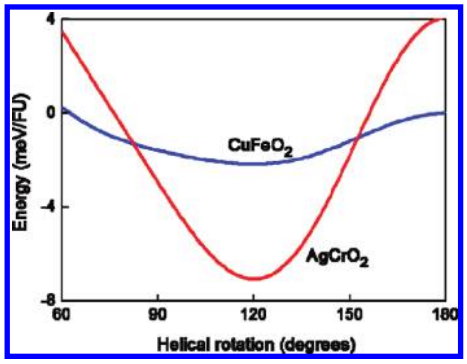

Figure 4. Plots of the spin exchange energy $E(\theta)$, per FU, of the helical spiral-spin structure Q_{a+b} = (q, q) calculated as a function of the helical rotation angle θ = q × 360° for $CuFeO_2$ and $AgCrO_2$ using their spin exchange parameters J_1−J_4 reduced by the overestimation factor *f* = 3.24 for $CuFeO_2$ and by *f* = 1.42 for $AgCrO_2$.

The $E(\theta)$ vs θ curves have the minimum at θ = 120° (i.e., q = 1/3) for both $CuFeO_2$ and $AgCrO_2$. This prediction is in good agreement with experiment for $AgCrO_2$.[26,27] It should be noted that the potential well around θ = 120° is deep around θ = 120° for $AgCrO_2$ but is very shallow for $CuFeO_2$. To probe the origin of this difference, we calculate the spin exchange energies of their ↑↑↓↓, Q_{a+b} (q = 1/3, 1/4, 1/5), and ↑↑↑↓↓ states in terms of their spin exchange parameters. The results of these calculations, summarized in Table 1, reveal that the ↑↑↓↓ state is less stable than the Q_{a+b} (q = 1/3) state in both $CuFeO_2$ and $AgCrO_2$. However, the ↑↑↓↓ state is much closer in energy to the Q_{a+b} (q = 1/3) state for $CuFeO_2$ than for $AgCrO_2$. Table 1 shows that the Q_{a+b} (q = 1/3) state is more stable than the ↑↑↓↓ state by

$$\Delta E = (-0.50J_1 + 2J_2 - 0.50J_3 - 0.33J_4)(N^2/4) \qquad (5)$$

where *N* = 5 for $CuFeO_2$ and *N* = 3 for $AgCrO_2$. Thus, ΔE is large for $AgCrO_2$ due to the strong AFM J_4 and the FM J_2, while ΔE is small for $CuFeO_2$ due to the weak AFM J_4 and the AFM J_2.

Since the Q_{a+b} (q = 1/3) and ↑↑↓↓ states of $CuFeO_2$ are close in energy, the extrinsic factors such as oxygen vacancy and applied magnetic field might easily affect which state, Q_{a+b} (q = 1/3) or ↑↑↓↓, $CuFeO_2$ adopts. It has been suggested that an O vacancy in a FeO_2 layer creates Fe^{2+} ions at the FeO_5 square pyramids

dx.doi.org/10.1021/cm2011567 |*Chem. Mater.* XXXX, XXX, 000–000

Table 1. Spin Exchange Energies (per FU) of the ↑↑↓↓, Q_{a+b} (q = 1/3, 1/4, 1/5), and ↑↑↑↓↓ states of $CuFeO_2$ and $AgCrO_2$ in Terms of Their Spin Exchange Parameters J_1-J_4

state	energy expression (per FU)[a]	$CuFeO_2$, meV/FU	$AgCrO_2$, meV/FU
↑↑↓↓	$(J_1 - J_2 + J_3 - 0.33J_4)(N^2/4)$	−1.58[b]	−2.94[c]
Q_{a+b} (q = 1/3)	$(1.50J_1 - 3J_2 + 1.50J_3)(N^2/4)$	−2.17	−7.01
Q_{a+b} (q = 1/4)	$(J_1 - J_2 + J_3 - 0.33J_4)(N^2/4)$	−1.58	−2.94
Q_{a+b} (q = 1/5)	$(0.19J_1 + 0.62J_2 + 1.31J_3 - 0.87J_4)(N^2/4)$	−0.77	+0.88
↑↑↑↓↓	$(0.20J_1 + 0.20J_2 + J_3 - 0.87J_4)(N^2/4)$	−0.49	+0.94

[a] $N = 5$ for $CuFeO_2$, and $N = 3$ for $AgCrO_2$. [b] Using the J_1-J_4 values reduced by the overestimation factor $f = 3.24$ (see the text). [c] Using the J_1-J_4 values reduced by the overestimation factor $f = 1.42$ (see the text).

around the vacancy site, and the uniaxial magnetism of such Fe^{2+} ions[28,29] provides a driving force for the surrounding Fe^{3+} ions to orient their moments along the *c*-axis leading to the ↑↑↓↓ state. An applied magnetic field tends to orient the moment of a magnetic ion perpendicular to the field when the field is not strong so that the Zeeman levels of the ion are almost equally populated. Thus, under such magnetic field applied along the *c*-axis, the spin orientation of $CuFeO_2$ would be governed by two competing factors: the oxygen-vacancy effect favoring the //c-spin orientation and the magnetic-field effect favoring the ⊥c-spin orientation. Then, the adoption of the helical spiral-spin structure under magnetic field $\mathbf{H} \approx 7-13$ T implies that the magnetic-field effect overcomes the oxygen-vacancy effect, so the intra- and interlayer spin frustration of $CuFeO_2$ is reduced by adopting the helical spiral-spin structure, as found for $AgCrO_2$. The occurrence of the ↑↑↑↓↓ structure under $\mathbf{H} > \sim 13$ T suggests that the energy gap between adjacent Zeeman levels of the Fe^{3+} ion become large, so only the lower-lying Zeeman levels are preferentially populated, thereby resulting in more moments parallel to the field direction.

5. CONCLUDING REMARKS

The spin exchanges of $CuFeO_2$ are frustrated, as found for $AgCrO_2$, but the two systems differ; the AFM interlayer exchange J_4 is strong in $AgCrO_2$ but weak in $CuFeO_2$, and the intralayer exchange J_2 is FM in $AgCrO_2$ but AFM in $CuFeO_2$. In contrast to the case of $AgCrO_2$, therefore, the ↑↑↓↓ state is only slightly higher in energy than the helical spiral-spin state Q_{a+b} (q = 1/3) in $CuFeO_2$ so that extrinsic factors such as oxygen vacancy and applied magnetic field can influence whether it adopts the ↑↑↓↓ or Q_{a+b} (q = 1/3) structure.

AUTHOR INFORMATION

Corresponding Author

*E-mail: mike_whangbo@ncsu.edu.

ACKNOWLEDGMENT

The research was supported by the Office of Basic Energy Sciences, Division of Materials Sciences, U.S. Department of Energy, under Grant No. DE-FG02- 86ER45259, and also by computing resources at the NERSC and the HPC Centers.

REFERENCES

(1) (a) Ederer, C.; Spaldin, N. A. *Curr. Opin. Solid State Mater. Sci.* **2005**, *9*, 128. (b) Ramesh, R.; Spaldin, N. A. *Nat. Mater.* **2007**, *6*, 21. (c) Khomskii, D. *Physics* **2009**, *2*, 20. (d) Dawber, M.; Rabe, K. M.; Scott, J. F. *Rev. Mod. Phys.* **2005**, *77*, 1083. (e) Eerenstein, W.; Mathur, N. D.; Scott, J. F. *Nature (London)* **2006**, *442*, 759. (f) Cheong, S. W.; Mostovoy, M. *Nat. Mater.* **2007**, *6*, 13. (g) Tokura, Y. *Science* **2006**, *312*, 1481.

(2) Kan, E.; Xiang, H.; Lee, C.; Wu, F.; Yang, J. L.; Whangbo, M. *Angew. Chem., Int. Ed.* **2010**, *49*, 1603.

(3) (a) Mostovoy, M. *Phys. Rev. Lett.* **2006**, *96*, 067601. (b) Yamasaki, Y.; Miyasaka, S.; Kaneko, Y.; He, J.-P.; Arima, T.; Tokura, Y. *Phys. Rev. Lett.* **2006**, *96*, 207204. (c) Sergienko, I.; Sen, C.; Dagotto, E. *Phys. Rev. Lett.* **2006**, *97*, 227204. (d) Fiebig, M. *J. Phys. D* **2005**, *38*, R123. (e) Kimura, T.; Goto, T.; Shintani, H.; Ishizaka, K.; Arima, T.; Tokura, Y. *Nature (London)* **2003**, *426*, 55. (f) Hur, N.; Park, S.; Sharma, P. A.; Ahn, J. S.; Guha, S.; Cheong, S.-W. *Nature (London)* **2004**, *429*, 392.

(4) (a) Chapon, L. C.; Radaelli, P. G.; Blake1, G. R.; Park, S.; Cheong, S.-W. *Phys. Rev. Lett.* **2006**, *96*, 097601. (b) Choi, Y. J.; Yi, H. T.; Lee, S.; Huang, Q.; Kiryukhin, V.; Cheong, S.-W. *Phys. Rev. Lett.* **2008**, *100*, 047601.

(5) (a) Xiang, H. J.; Whangbo, M.-H. *Phys. Rev. Lett.* **2007**, *99*, 257203. (b) Xiang, H. J.; Wei, S.-H.; Whangbo, M.-H.; Da Silva, J. L. F. *Phys. Rev. Lett.* **2008**, *101*, 037209. (c) Zhang, Y.; Xiang, H. J.; M.-H. Whangbo, M.-H. *Phys. Rev. B* **2009**, *79*, 054432. (d) Malashevich, A.; Vanderbilt, D. *Phys. Rev. Lett.* **2008**, *101*, 037210. (e) Katsura, H.; Nagaosa, N.; Balatsky, A. V. *Phys. Rev. Lett.* **2005**, *95*, 057205.

(6) (a) Kimura, T.; Lashley, J. C.; Ramirez, A. P. *Phys. Rev. B* **2006**, *73*, 220401(R). (b) Nakajima, T.; Mitsuda, S.; Kanetsuki, S.; Prokes, K.; Podlensnyak, A.; Kimura, H.; Noda, Y. *J. Phys. Soc. Jpn.* **2007**, *76*, 043709. (c) Arima, T. *J. Phys. Soc. Jpn.* **2007**, *76*, 073702.

(7) (a) Seki, S.; Onose, Y.; Tokura, Y. *Phys. Rev. Lett.* **2008**, *101*, 067204. (b) Kan, E. J.; Xiang, H. J.; Zhang, Y.; Lee, C.; Whangbo, M.-H. *Phys. Rev. B* **2009**, *80*, 104417.

(8) (a) Prewitt, C. T.; Shannon, R. D.; Rogers, D. B. *Inorg. Chem.* **1971**, *10*, 719. (b) Pabst, A. *Am. Mineral.* **1946**, *31*, 539. (c) Soller, W.; Thompson, A. J. *Phys. Rev.* **1935**, *47*, 644.

(9) Gehle, E.; Sabrowsky, H. *Z. Naturforsch., B: Anorg. Chem. Org. Chem.* **1975**, *30*, 659.

(10) (a) Doumerc, J.-P.; Wichainchai, A.; Ammar, A.; Pouchard, M.; Hagenmuller, P. *Mater. Res. Bull.* **1986**, *21*, 745. (b) El Ataoui, K.; Doumerc, J.-P.; Ammar, A.; Fournès, L.; Wattiaux, A.; Grenier, J.-C.; Pouchard, M. *J. Alloys Comp.* **2004**, *368*, 79.

(11) Mitsuda, S.; Mase, M.; Prokes, K.; Kitazawa, H.; Katori, H. A. *J. Phys. Soc. Jpn.* **2000**, *69*, 3513.

(12) (a) Mitsuda, S.; Mase, M.; Prokes, K.; Kitazawa, H.; Aruga Katori, H. *J. Phys. Soc. Jpn.* **2000**, *69*, 3513. (b) Petrenko, O. A.; Balakrishnan, G.; Lees, M. R.; Paul, D. McK.; Hoser, A. *Phys. Rev. B* **2000**, *62*, 8983.

(13) (a) Kanetsuki, S.; Mitsuda, S.; Nakajima, T.; Anazawa, D.; Katori, H. A.; Prokes, K. *J. Phys.: Condens. Matter* **2007**, *19*, 145244. (b) Seki, S.; Yamasaki, Y.; Shiomi, Y.; Iguchi, S.; Onose, Y.; Tokura, Y. *Phys. Rev. B* **2007**, *75*, 100403(R). (c) Terada, N.; Nakajima, T.; Mitsuda, S.; Kitazawa, H.; Kaneko, K.; Metoki, N. *Phys. Rev. B* **2008**, *78*, 014101.
(d) Mitsuda, S.; Nakajima, T.; Yamano, M.; Takahashi, K.; Yamazaki, H.; Masuda, K.; Kaneko, Y.; Terada, N.; Prokes, K.; Kiefer, K. *Phys. B* **2009**, *404*, 2532.

(14) Ye, F.; Fernandez-Baca, J. A.; Fishman, R. S.; Ren, Y.; Kang, H. J.; Qiu, Y.; Kimura, T. *Phys. Rev. B* **2007**, *99*, 157201.

(15) (a) Fishman, R. S. *J. Appl. Phys.* **2008**, *103*, 07B109. (b) Fishman, R. S.; Ye, F.; Fernandez-Baca, J. A.; Haraldsen, J. T.; Kimura, T. *Phys. Rev. B* **2008**, *78*, 140407(R). (c) Haraldsen, J. T.; Ye, F.; Fishman, R. S. *Phys. Rev. B* **2010**, *82*, 144441.

(16) (a) Terada1, N.; Narumi, Y.; Sawai, Y.; Katsumata, K.; Staub, U.; Tanaka, Y.; Kikkawa, A.; Fukui, T.; Kindo, K.; Yamamoto, T.; Kanmuri, R.; Hagiwara, M.; Toyokawa, H.; Ishikawa, T.; Kitamura1, H. *Phys. Rev. B* **2007**, *75*, 224411. (b) Lummen, T. T. A.; Strohm, C.; Rakoto, H.; Nugroho, A. A.; van Loosdrecht, P. H. M. *Phys. Rev. B* **2009**, *80*, 012406. (c) Lummen, T. T. A.; Strohm, C.; Rakoto, H.; van Loosdrecht, P. H. M. *Phys. Rev. B* **2010**, *81*, 224420. (d) Ye, Fe.; Ren, Y.; Huang, Q.; Fernandez-Baca, J. A.; Dai, P.; Lynn, J. W.; Kimura, T. *Phys. Rev. B* **2006**, *73*, 220404. (e) Eyert, V.; Frésard, R.; Maignan, A. *Phys. Rev. B* **2008**, *78*, 052402. (f) Malvestuto, M.; Bondino, F.; Magnano, E.; Lummen, T. T. A.; van Loosdrecht, P. H. M.; Parmigiani, F. *Phys. Rev. B* **2011**, *83*, 134422. (g) Plumer, M. L. *Phys. Rev. B* **2007**, *76*, 144411. (h) Plumer, M. L. *Phys. Rev. B* **2008**, *78*, 094402. (i) Quirion, G.; Tagore, M. J.; Plumer, M. L.; Petrenko, O. A. *Phys. Rev. B* **2008**, *77*, 094111.

(17) (a) Blöchl, P. E. *Phys. Rev. B* **1994**, *50* (17), 953. (b) Kresse, G.; Joubert, D.**1999**, *59*, 1758.

(18) Kresse, G.; Furthmüller *J. Comput. Mater. Sci.* **1996**, *6*, 15. *Phys. Rev. B* **1996**, *54*, 11169.

(19) Perdew, J. P.; Burke, S.; Ernzerhof, M. *Phys. Rev. Lett.* **1996**, *77*, 3865.

(20) (a) Dai, D.; Whangbo, M.-H. *J. Chem. Phys.* **2001**, *114*, 2887. (b) Dai, D.; Whangbo, M.-H. *J. Chem. Phys.* **2003**, *118*, 29. (c) Whangbo, M.-H.; Koo, H.-J.; Dai, D. *J. Solid State Chem.* **2003**, *176*, 417.

(21) (a) Greedan, J. E. *J. Mater. Chem.* **2001**, *11*, 37. (b) Dai, D.; Whangbo, M.-H. *J. Chem. Phys.* **2004**, *121*, 672.

(22) (a) Xiang, H. J.; Lee, C.; Whangbo, M.-H. *Phys. Rev. B: Rapid Commun.* **2007**, *76*, 220411(R). (b) Koo, H.-J.; Whangbo, M.-H. *Inorg. Chem.* **2008**, *47*, 128. (c) Koo, H.-J.; Whangbo, M.-H. *Inorg. Chem.* **2008**, *47*, 4779.

(23) Smart, J. S. *Effective Field Theory of Magnetism*; Saunders: Philadelphia, 1966.

(24) Takeda, K.; Miyake, K.; Hitaka, M.; Kawae, T.; Ysguchi, N.; Mekata, M. *J. Phys. Soc. Jpn.* **1994**, *63*, 2017.

(25) Olveira, G. N. P.; Lopes, A. M. L.; Mendonça, T. M.; Araújo, J. P.; Moreira, J. A.; Almeida, A.; Amaral, V. S.; Correia, J. G. *Hyperfine Interact.* **2010**, *197*, 123.

(26) Oohara, Y.; Mitsuda, S.; Yoshizawa, H.; Yaguchi, N.; Kuriyama, H.; Asana, T.; Mekata, M. *J. Phys. Soc. Jpn.* **1994**, *63*, 847.

(27) Seki, S.; Onose, Y.; Tokura, Y. *Phys. Rev. Lett.* **2008**, *101*, 067204.

(28) Whangbo, M.-H.; Dai, D.; Lee, K.-S.; Kremer, R. K. *Chem. Mater.* **2006**, *18*, 1266.

(29) Dai, D.; Whangbo, M.-H. *Inorg. Chem.* **2005**, *44*, 4407.